

E3 ligase MKRN2 destabilizes PPP2CA proteins to inactivate canonical Wnt pathway and mitigates tumorigenesis of clear cell renal cell carcinoma

Tiexi Yu^{a,b,c,*}, Weiquan Li^{a,b,c,*}, Xiangui Meng^{a,b,c,*}, Hongwei Yuan^{a,b,c}, Hailong Ruan^{a,b,c,#}, Wen Xiao^{a,b,c,#}, Xiaoping Zhang^{a,b,c,#}

* Tiexi Yu, Weiquan Li, and Xiangui Meng contributed equally to this work

Correspondence:

Hailong Ruan hluan2010@126.com

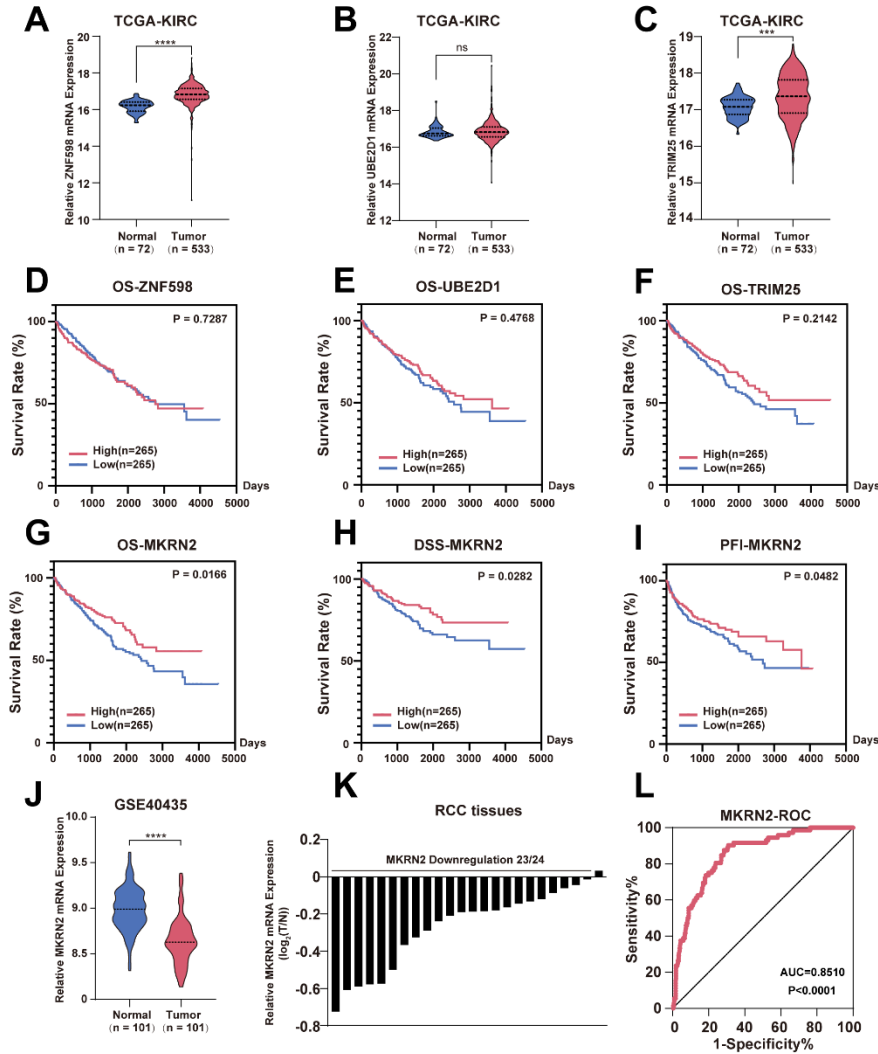
Wen Xiao wxuro20@hust.edu.cn

Xiaoping Zhang xzhang@hust.edu.cn

^aDepartment of Urology, Union Hospital, Tongji Medical College, Huazhong University of Science and Technology, Wuhan, 430022, China.

^bShenzhen Huazhong University of Science and Technology Research Institute, Shenzhen 518000, China.

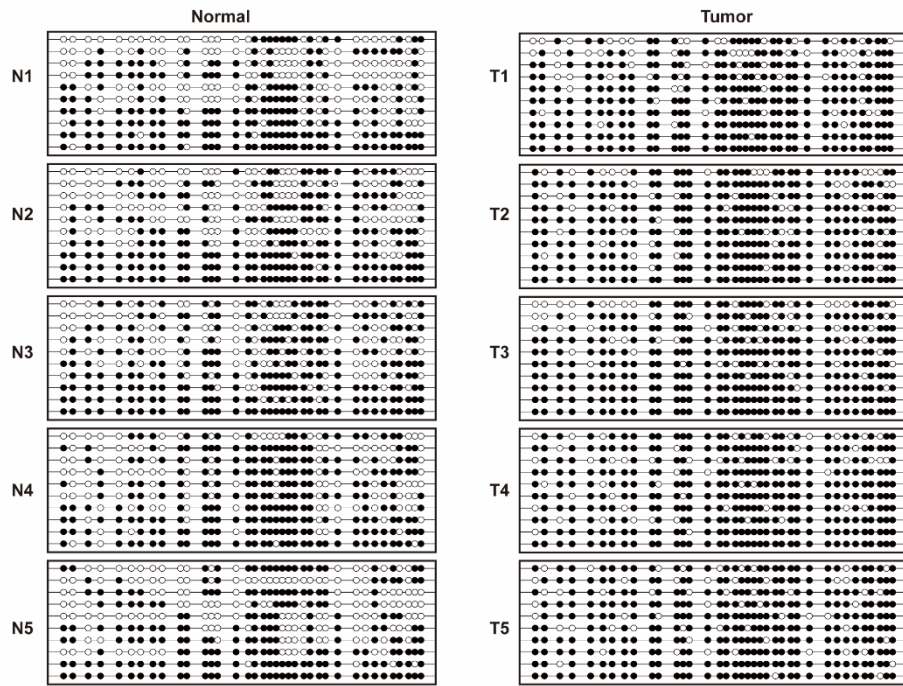
^cInstitute of Urology, Tongji Medical College, Huazhong University of Science and Technology, Wuhan 430022, China.



Supplementary Fig. 1: MKRN2 is down-regulated in ccRCC

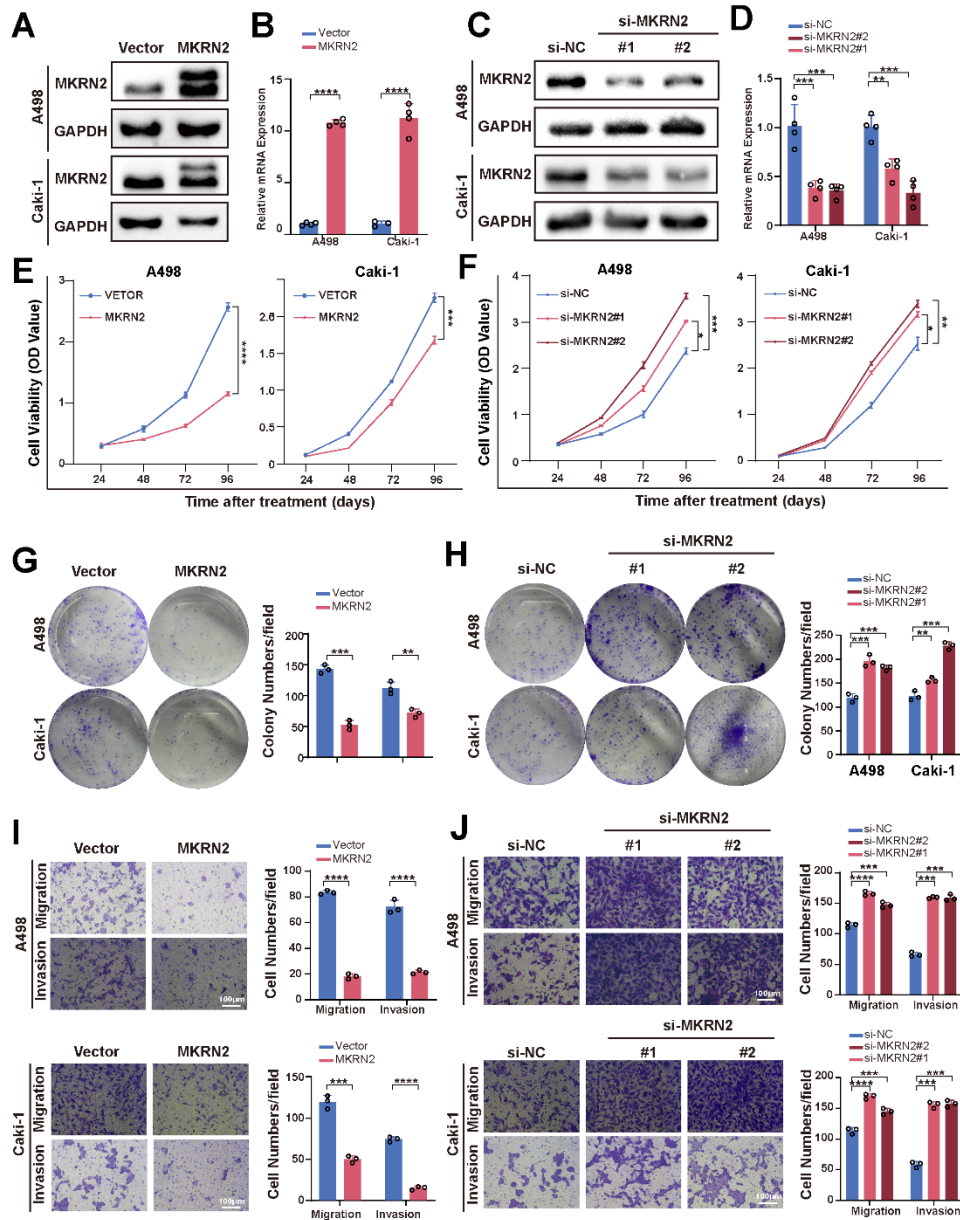
(A, B, C) The expression level of ZNF598, UBE2D1 and TRIM25 in TCGA-KIRC dataset. (D, E, F, G) The Kaplan-Meier analyses of the association between the overall survival rate of ccRCC patients and the expression levels of ZNF598, UBE2D1, TRIM25 and MKRN2. (H) The disease specific survival of patients in high and low expression level of MKRN2. (I) The progression free interval of patients in n high and low expression level of MKRN2. (J) The expression level of MKNR2 in ccRCC from GSE40435 dataset. (K) The mRNA levels of MKRN2 in ccRCC tissues and paired adjacent normal tissues from 24 patients. (L) ROC curve of MKRN2 in ccRCC from TCHA-KIRC dataset.

A

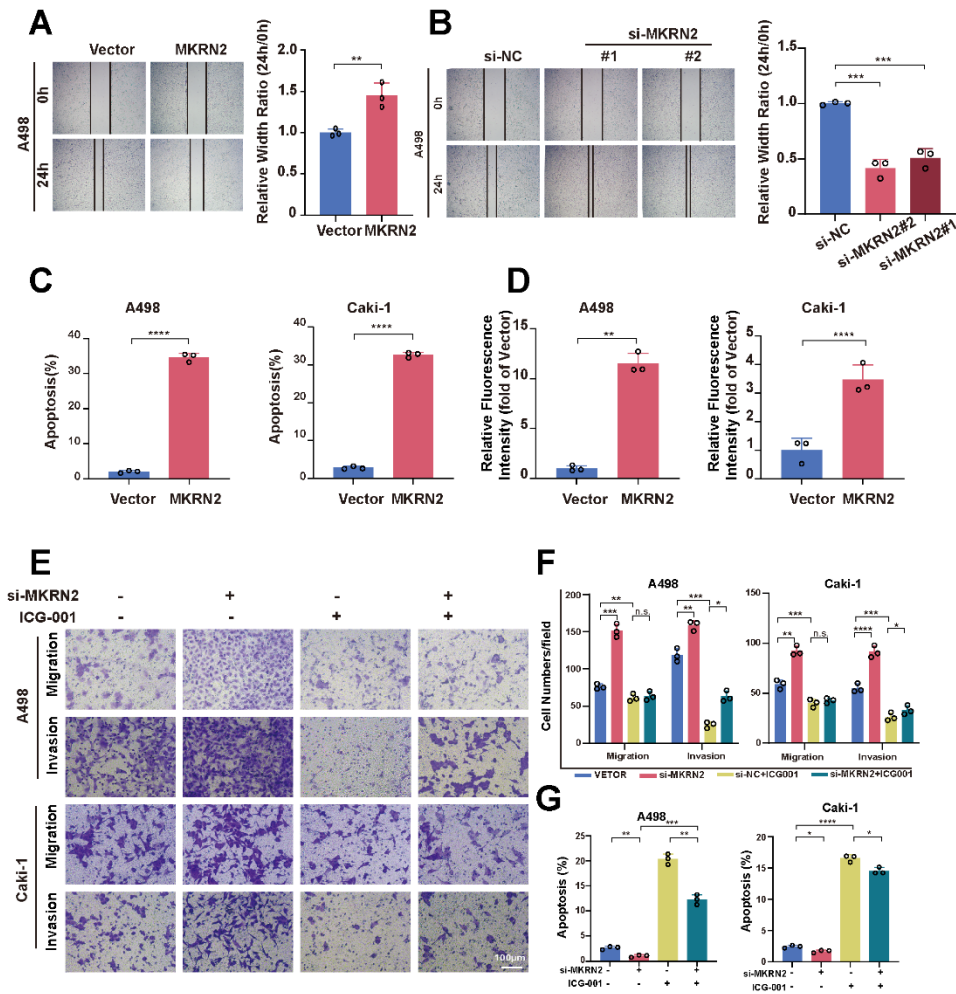


Supplementary Fig. 2: DNA methylation caused the low expression of MKRN2 in ccRCC.

(A) BSP results of MKRN2 methylation status in adjacent tissues (N) and ccRCC tissues (T).

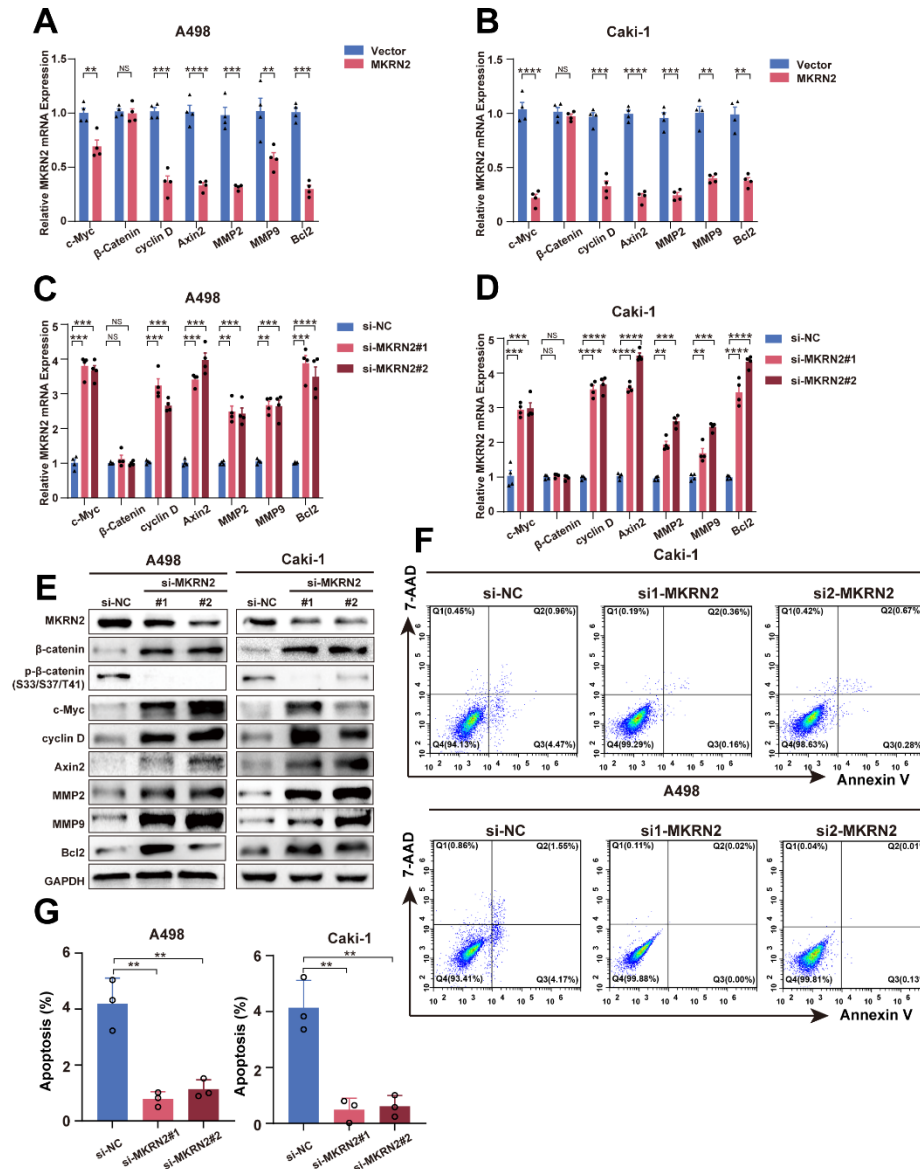


Supplementary Fig. 3: MKRN2 demonstrated a suppressive effect on the in vitro progression of ccRCC. (A, B, C, D) MKRN2-overexpressing or MKRN2-knockdown ccRCC cell lines were established by transfecting overexpressing lentivirus and siRNA. (E, F) Cell growth curves were generated through CCK8 assays for the specified cells (n = 3). (G, H) Colony formation assays were conducted for the indicated ccRCC cells (n = 3). (I, J) Migration and invasion assays were performed for the specified ccRCC cells (n = 3). Significance levels denoted as follows: ****p < .0001, ***p < .001, **p < .01, and *p < .05.



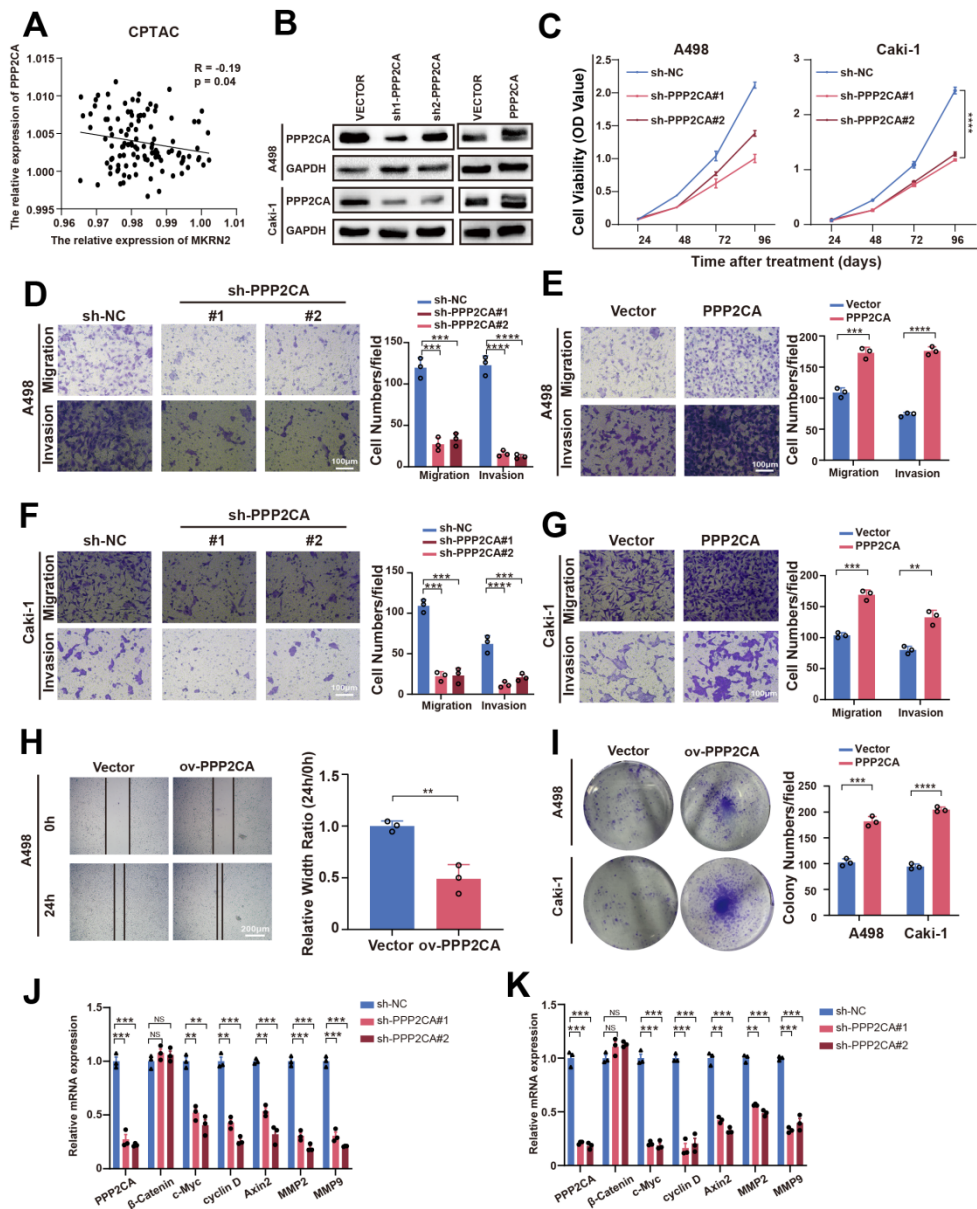
Supplementary Fig. 4: MKRN2 repressed Wnt signaling pathways activation and tumor progression.

(A, B) Wound healing assay were generated for the A498 cells with MKRN2 overexpression and knock down (n = 3). (C) The apoptosis rate for the cells with MKRN2-overexpression (n = 3). (D) The relative fluorescence intensity of TUNEL for the cells with MKRN2-overexpression (n = 3). (E, F) The relative cell number of the migration and invasion assays for the specified cells (n = 3). Cells with MKRN2 knockdown were treated with 10 μ M ICG-001 (an inhibitor of β -catenin/TCF) or DMSO. (G) The apoptosis rate for the cells for the specified cells (n = 3). Significance levels denoted as follows: ****p < .0001, ***p < .001, **p < .01, and *p < .05.



Supplementary Fig. 5: MKRN2 inhibited the activation of Wnt signaling pathway.

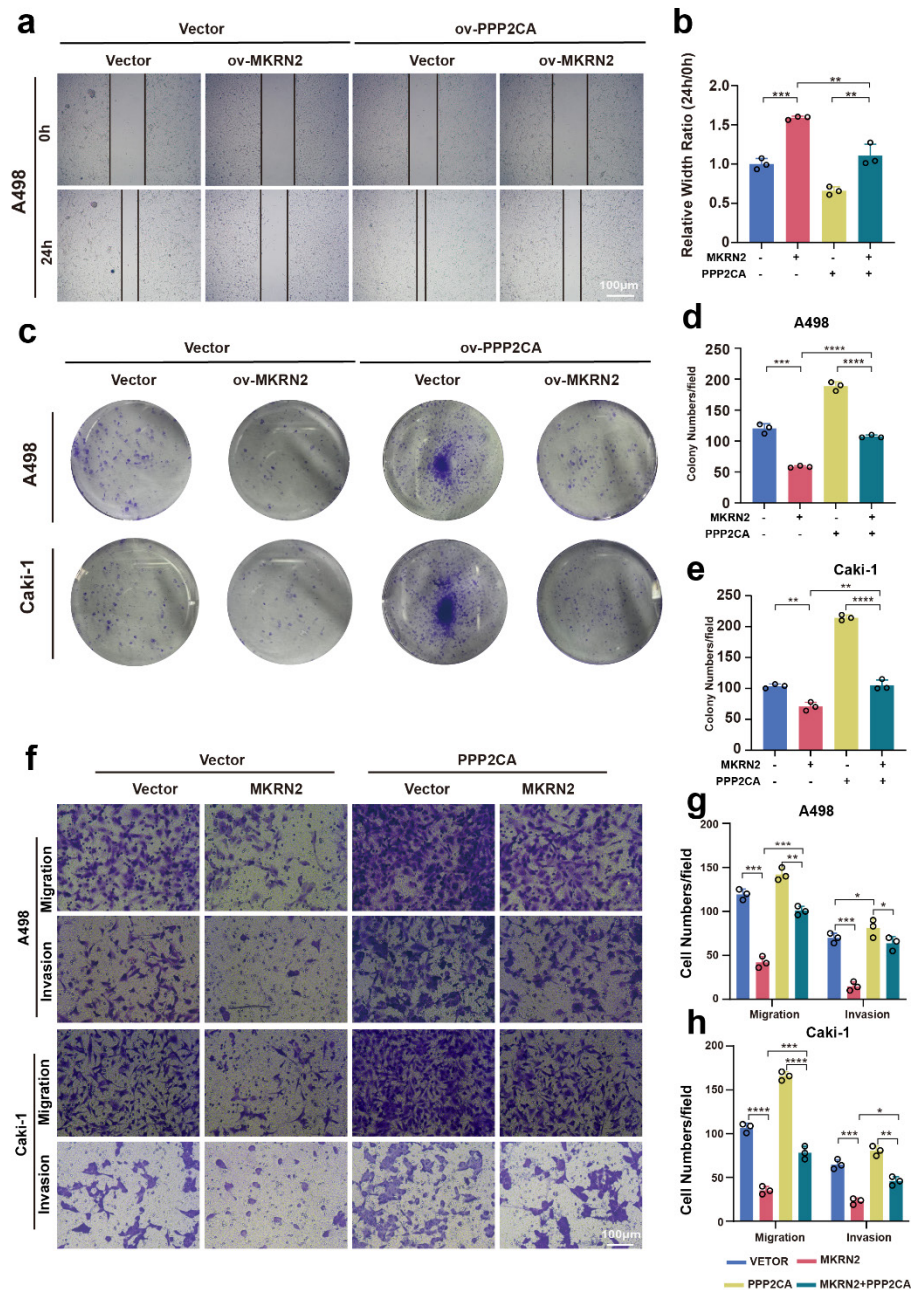
(A, B) Relative mRNA expression of wnt related genes for the cells with MKRN2-overexpression (n = 4). (C, D) Relative mRNA expression of wnt related genes for the cells with MKRN2-knockdown (n = 4). (E) Protein expression of wnt related genes for the cells with MKRN2-knockdown (n = 3). (F) Flow cytometry analysis was employed to determine the proportion of apoptotic cells in samples with MKRN2 knockdown compared to control cells (n = 3). (G) The apoptosis rate in the MKRN2 knock down cell lines (n = 3). Significance levels denoted as follows: ****p < .0001, ***p < .001, **p < .01, and *p < .05.



Supplementary Fig. 6: PPP2CA played an oncogenic role in ccRCC.

(A) **MKRN2** proteins had a negative correlation with PPP2CA proteins in ccRCC. (B) PPP2CA-overexpressing or PPP2CA-knockdown ccRCC cell lines were established by transfecting overexpressing lentivirus and siRNA. (C-G) CCK8 and Transwell assay for the indicated cells. And

the relative cell number of the migration and invasion assays for the cells with PPP2CA-overexpression or sh-PPP2CA (n = 3). (H) Wound healing assay for the cells with PPP2CA-overexpression (n = 3). (I) Colony assay for the cells with PPP2CA-overexpression (n = 3). (J)-(K) mRNA level of Wnt signing effected by sh-PPP2CA. Significance levels denoted as follows: ****p < .0001, ***p < .001, **p < .01, and *p < .05.



Supplementary Fig. 7: MKRN2 inhibited ccRCC progression through PPP2CA in vitro.

(A) Wound healing assay were generated for the specified cells. (B) The relative width ratio of wound healing assay for for the specified cells. (n = 3). (C) Colony assay for the specified cells. (D,

E) The colony numbers for the cells with PPP2CA-overexpression (n = 3). (F, G, H) Migration and invasion assays were conducted for the indicated ccRCC cells (n = 3) (Magnification: 200×). Significance levels denoted as follows: ****p < .0001, ***p < .001, **p < .01, and *p < .05.

Supplementary table 1

| First antibodies : | Brand | Cat No. | Dilution |
|---|-------------|------------|------------------------|
| anti-DDDDK-Tag | Abclonal | AE169PM | 1:1000 |
| anti-Myc-Tag | Abclonal | AE010 | 1:1000 |
| anti-Phospho-B-Catenin-S29/33/37/T41 | Abclonal | AP1076 | 1:500 |
| anti-Phospho-B-Catenin-S552 | Abclonal | AP1315 | 1:1000 |
| anti-Bcl-2 | Abclonal | A19693 | 1:1000 |
| anti-MMP2 | Abclonal | A19080 | 1:1000 |
| anti-MMP9 | Abclonal | A26079 | 1:1000 |
| anti-PPP2CA | Abclonal | A6702 | Wb: 1:1000 IF: 1:50 |
| anti-β-Catenin | Proteintech | 51067-2-AP | Wb:1:1000 IF: 1:100 |
| anti-β-Catenin | Abclonal | A19657 | 1:2000 |
| anti-MKRN2 | Santa Cruze | sc-101118 | Wb: 1:100 IF: 1:100 |
| anti-Axin2 | Abclonal | A2513 | 1:2000 |
| anti-PPP2R1A | Abclonal | A18571 | 1:1000 |
| anti-Cyclin D | Abclonal | A19038 | 1:1000 |
| | | | |
| Secend antibodies: | | | |
| HRP Goat Anti-Rabbit IgG (H+L) | Abclonal | AS014 | 1:3000 |
| HRP Goat Anti-Mouse IgG (H+L) | Abclonal | AS003 | 1:3000 |
| Dylight 488, Goat Anti-Rabbit IgG | abcam | ab96899 | IF: 1:100 |
| Dylight 549, Goat Anti-Rabbit IgG | abcam | ab96885 | IF: 1:100 |
| Dylight 488, Goat Anti-Mouse IgG | abcam | ab96879 | IF: 1:100 |
| Dylight 549, Goat Anti-Mouse IgG | abcam | ab96881 | IF: 1:100 |
| CoraLite647-conjugated Goat AntiMouse IgG | Proteintech | SA00014-10 | IF: 1:200 |

Supplementary table 2

| Symbol | Sequence | NCBI accession numbers | Lengths |
|--------|----------|------------------------|---------|
|--------|----------|------------------------|---------|

| | | | |
|----------|-------------------------|----------------|-----|
| MKRN2-F | AGGAAGTCAGTGCCTATTCTCA | NM_014160.5 | 111 |
| MKRN2-R | TGGTCATATCTGCACCGAGTT | | |
| | | | |
| PPP2AC-F | CAAAAGAATCCAACGTGCAAGAG | NM_002715.4 | 211 |
| PPP2AC-R | CGTTCACGGTAACGAACCTT | | |
| | | | |
| BCL2-F | GGTGGGGTCATGTGTGTGG | NM_000657.3 | 89 |
| BCL2-R | CGGTTCAGGTACTCAGTCATCC | | |
| | | | |
| KI67-F | ACGCCTGGTTACTATCAAAAGG | NM_002417.5 | 209 |
| KI67-R | CAGACCCATTTACTTGTGTTGGA | | |
| | | | |
| MMP9-F | TGTACCGCTATGGTTACACTCG | NM_004994.3 | 97 |
| MMP9-R | GGCAGGGACAGTTGCTTCT | | |
| | | | |
| MMP2-F | TACAGGATCATTGGCTACACACC | NM_004530.6 | 90 |
| MMP2-R | GGTCACATCGCTCCAGACT | | |
| | | | |
| CCND1-F | GCTGCGAAGTGGAACCATC | NM_053056.3 | 135 |
| CCND1-R | CCTCCTTCTGCACACATTTGAA | | |
| | | | |
| CTNNB1-F | AAAGCGGCTGTTAGTCACTGG | XM_047447479.1 | 215 |
| CTNNB1-R | CGAGTCATTGCATACTGTCCAT | | |
| | | | |
| CMYC-F | GGCTCCTGGCAAAAGGTCA | NM_002467.6 | 119 |
| CMYC-R | CTGCGTAGTTGTGCTGATGT | | |